

# Design of X-Band Integrated Filtering Pyramidal Horn Antenna

Yun Wang\*, Fu-Chang Chen, and Qing-Xin Chu

**Abstract**—An X-band pyramidal horn antenna with a fourth order Chebyshev filtering function is presented in this paper. Four resonators are implemented in linear rectangular waveguide in the filter design. The last stage resonator provides not only resonance pole but also radiation function. To achieve high directivity, a pyramidal horn is attached to the filter output port, with negligible effect on the filter performance. Theoretical results are calculated based on the coupling matrix between the resonators. Finally, a pyramidal horn antenna operating at 10 GHz is designed and fabricated for demonstration. The measured results have found to be in good agreement with the simulated ones.

## 1. INTRODUCTION

X-band wireless communication systems are widely applied in different fields, such as radar, space, and satellite communications. In these systems, both filters and antennas are most common individual components. It means that a matching circuit is needed between them. The systems usually occupy too much space. Hence, there has been some demand to integrate them in a single component, which is called filtering antenna, to omit matching design and reduce size.

Recently, there has been great interest among researchers in designing antennas with filtering function [1–12]. Antennas combined with cavity filters using a substrate integrated waveguide (SIW) technique were proposed in [1–3]. In [4–10], the authors used the method of filter synthesis to design filtering antennas since the antenna unit served as a radiator as well as one of the resonators. The antenna units were designed in various forms, such as U-shape [4, 5],  $\Gamma$ -shape [6], and fan-shape [7]. An approach of X-band waveguide antenna with integrated filter was presented in [8]. X-band waveguide planar filtering antenna arrays using an all-resonator structure was reported in [11] and [12], where the coupling matrix was calculated to deduce the physical dimensions.

Typically, a horn antenna is a broadband radiator. Its frequency range is bounded by cutoff frequencies of the first two modes provided by the feeding waveguide [13]. However, we require narrow band response in some fields such as radar and satellite communications in order to reduce noise interference. To solve this problem, waveguide horn antennas with microstrip filters integrated were presented in [14, 15]. But the in-band characteristics are not good enough, and the horns take up too much space.

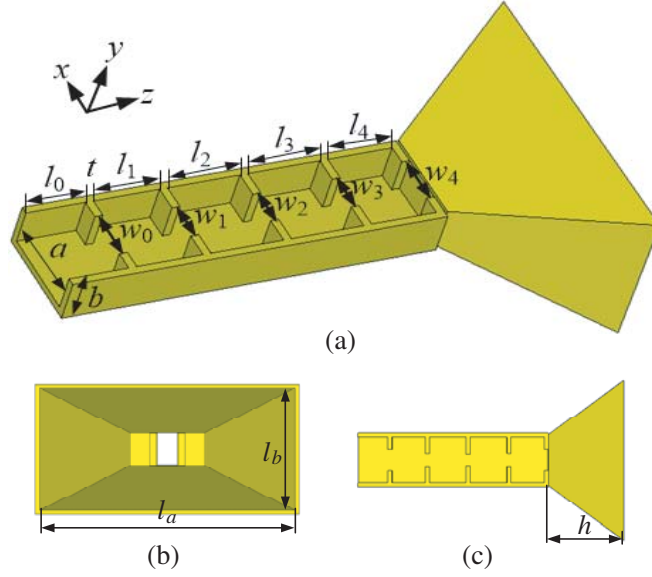
This letter presents a filtering pyramidal horn antenna. As depicted in Fig. 1(a), it comprises four cavity resonators in the rear of the horn, while the last stage resonator also acts as a radiator. The resonators are coupled through the inductive iris. Fabrication and measurement are illustrated. The proposed antenna operates at X-band 10 GHz with a fourth order Chebyshev filtering response with fractional bandwidth (FBW) of 2%.

---

*Received 5 November 2018, Accepted 13 January 2019, Scheduled 2 March 2019*

\* Corresponding author: Yun Wang (yunwang@scut.edu.cn).

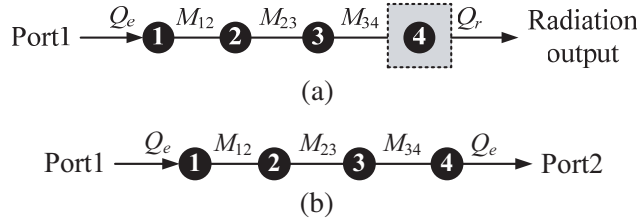
The authors are with the School of Electronic and Information Engineering, South China University of Technology, Guangzhou, China.



**Figure 1.** Geometry of the proposed pyramidal antenna with top cover removed. (a) Perspective view. (b) Side view. (c) Top view.  $a = 22.86$ ,  $b = 10.16$ ,  $l_0 = 15$ ,  $l_1 = 16.76$ ,  $l_2 = 18.49$ ,  $l_3 = 18.48$ ,  $l_4 = 16.69$ ,  $w_0 = 10.86$ ,  $w_1 = 6.78$ ,  $w_2 = 6.25$ ,  $w_3 = 6.79$ ,  $w_4 = 10.85$ ,  $l_a = 78.81$ ,  $l_b = 38.38$ ,  $h = 37.5$ ,  $t = 2$ . Unit: mm.

## 2. FILTER SYNTHESIS AND HORN DESIGN

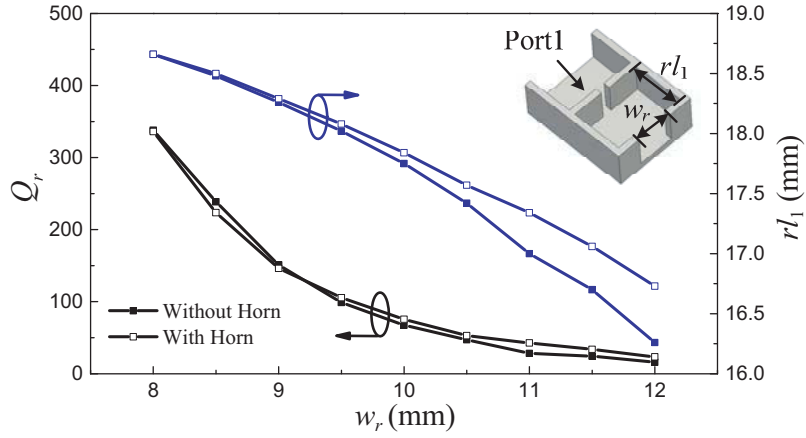
Figure 2(a) shows the coupling topology of the proposed antenna. The symbols  $Q_e$  and  $Q_r$  are the external quality factor of the input resonator and the radiation quality factor of the output resonator, respectively.  $M_{12}$ ,  $M_{23}$ , and  $M_{34}$  are the coupling coefficients between the adjacent resonators. Since the antenna is designed as the last resonator, the radiation output is equivalent to the output port of the relevant bandpass filter, as shown in Fig. 2(b). Thus,  $Q_r = Q_e$  is required. The value of  $Q_r$  can be extracted from the simulated magnitude of  $S_{11}$  response using a  $Q$ -calculation technique for a one-port component [16].



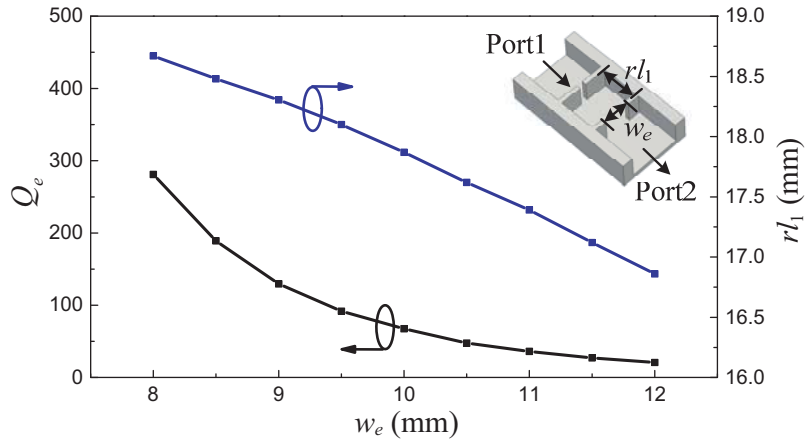
**Figure 2.** Coupling topology. (a) Proposed filtering antenna. (b) Relevant bandpass filter.

Figure 3 depicts the  $Q_r$  value of a single cavity resonator (embedded in Fig. 3) versus the aperture width ( $w_r$ ). The  $Q_r$  value is obtained from CST simulation software. When  $w_r$  increases, the  $Q_r$  value decreases. Thus, the radiation quality factor can be adjusted by controlling the width of the aperture. The  $Q_r$  value of the single cavity resonator with the proposed pyramidal horn is also plotted in Fig. 3 for comparison, which tells that radiation factor is insensitive to the additional horn. Fig. 4 depicts the extracted  $Q_e$  value versus the iris window width ( $w_e$ ). The dimension of  $w_e$  should be determined to meet the equation  $Q_r = Q_e$ , referring to Fig. 3 and Fig. 4.

In this design, a fourth order Chebyshev lowpass prototype with a return loss of  $-20$  dB and  $FBW$  of 2% is chosen. Equations between the values of the lumped elements and the normalized coupling



**Figure 3.** Radiation quality factor  $Q_r$  versus the value of  $w_r$ , while  $rl_1$  is adjusted to keep the center frequency at 10 GHz. (Horn dimensions:  $l_a = 78.81$  mm,  $l_b = 38.38$  mm,  $h = 37.5$  mm).



**Figure 4.** External quality factor  $Q_e$  versus the value of  $w_e$ , while  $rl_1$  is adjusted to keep the center frequency at 10 GHz.

coefficients and external/radiation quality factors can be listed as [17]:

$$m_{12} = M_{12}/FBW = 1/\sqrt{g_1g_2} \tag{1}$$

$$m_{23} = M_{23}/FBW = 1/\sqrt{g_2g_3} \tag{2}$$

$$m_{34} = M_{34}/FBW = 1/\sqrt{g_3g_4} \tag{3}$$

$$q_{e1} = q_{r4} = g_1 \tag{4}$$

where  $g_1, g_2, g_3,$  and  $g_4$  are the element values for the lowpass filter prototypes. The calculated results are  $q_{e1} = q_{r4} = 0.9314$  and

$$[m] = \begin{bmatrix} 0 & 0.9116 & 0 & 0 \\ 0.9116 & 0 & 0.7005 & 0 \\ 0 & 0.7005 & 0 & 0.9116 \\ 0 & 0 & 0.9116 & 0 \end{bmatrix}$$

Fig. 5 shows the extracted coupling coefficient between two adjacent cavity resonators. The extraction results play a guiding role in designing the width of iris window and the length of resonators of the proposed antenna.

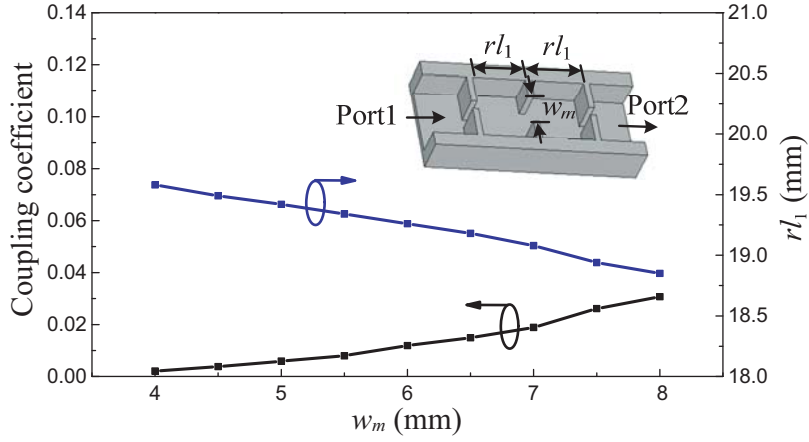


**Figure 5.** Coupling coefficient versus the value of  $w_m$ , while  $r_{l_1}$  is adjusted to keep the center frequency at 10 GHz.

According to Cozzens's method, the dimensions of the pyramidal horn, as shown in Figs. 1(b) and (c), can be obtained using the following formulas [18]:

$$l_a = 0.4675 * \lambda * \sqrt{\exp(0.2303 * G)} \quad (5)$$

$$l_b = 0.3463 * \lambda * \sqrt{\exp(0.2303 * G)} \quad (6)$$

$$h = k\lambda \quad (7)$$

where  $l_a$  and  $l_b$  are the  $H$ -plane ( $xz$ -plane) and  $E$ -plane ( $yz$ -plane) aperture lengths, respectively;  $h$  is the axial length;  $\lambda$  is the wavelength of the center frequency;  $G$  is the given antenna gain; and  $k$  is a coefficient determined by  $G$ . In our design, setting a gain of 15 dB, the coefficient  $k$  is 1.25 from the table in [15]. Thus, the original dimensions of the proposed horn are calculated to be  $l_a = 78.81$  mm,  $l_b = 58.38$  mm, and  $h = 37.5$  mm.

The simulated  $H$ -plane radiation patterns under different  $H$ -plane aperture lengths  $l_a$  is depicted in Fig. 6, and the  $E$ -plane radiation patterns under different  $E$ -plane aperture lengths  $l_b$  is depicted in Fig. 7. The results show that the directivity has little change with different  $l_a$ . But when  $l_b$  decreases, sidelobe decreases while beamwidth increases. Hence,  $l_b$  is chosen to be 38.38 mm in this work to obtain an optimized directivity and reduce antenna size.

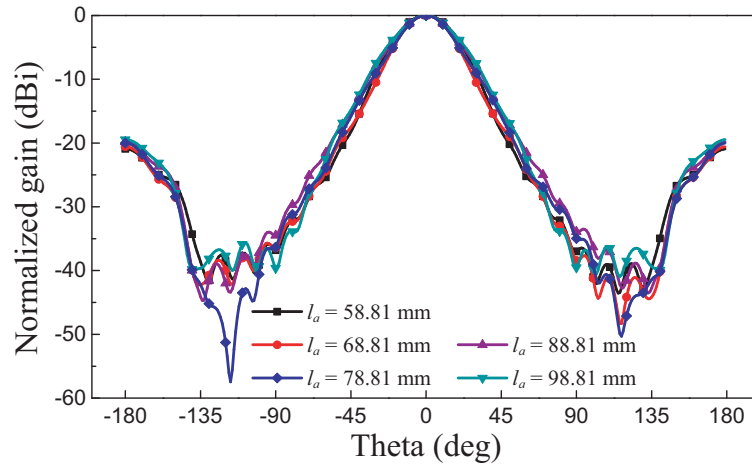


**Figure 6.** Simulated  $H$ -plane patterns of the proposed filtering horn antenna under different  $l_a$ .

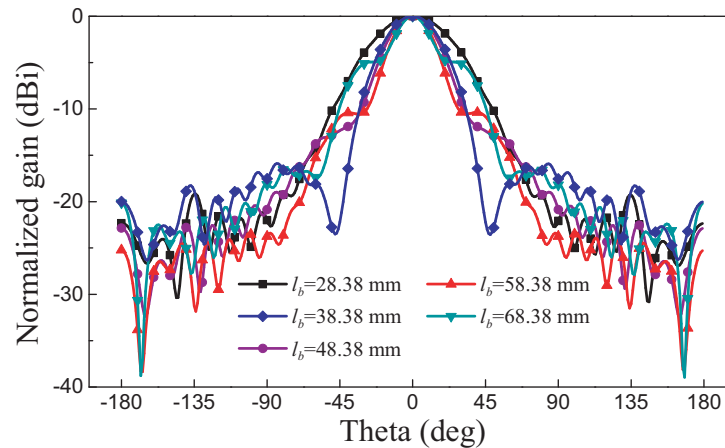


**Figure 7.** Simulated  $E$ -plane patterns of the proposed filtering horn antenna under different  $l_b$ .

### 3. SIMULATED AND EXPERIMENTAL RESULTS

The X-band filtering pyramidal horn antenna with optimized parameters listed in Fig. 1 is fabricated using aluminum alloy material for experimental verification. Full-wave simulation is carried out by CST software, and the measured  $S$ -parameter is characterized in HP N5230A network analyzer. Fig. 8 shows the simulated  $E$ -field magnitude distribution. Fig. 9 illustrates the simulated and measured reflection responses and realized radiation gain. It can be found that the results are in good agreement, and good filtering response is achieved. The measured center frequency is located at 10 GHz, and return loss is better than 14.55 dB in the passband from 9.88 GHz to 10.12 GHz. The measured radiation gain is compared with the simulated one in Fig. 9. It is observed that the filtering pyramidal horn antenna has a maximum gain of 14.45 dBi in simulation and 14.31 dBi in measurement at 10 GHz. Compared with the horn antenna without the filtering section, the selectivity of the gain is highly improved. A photograph of the fabricated antenna is shown in Fig. 10. The normalized co-polarization radiation patterns in  $H$ - and  $E$ -plane orientations are presented in Fig. 11. The measured sidelobe levels in  $H$ -

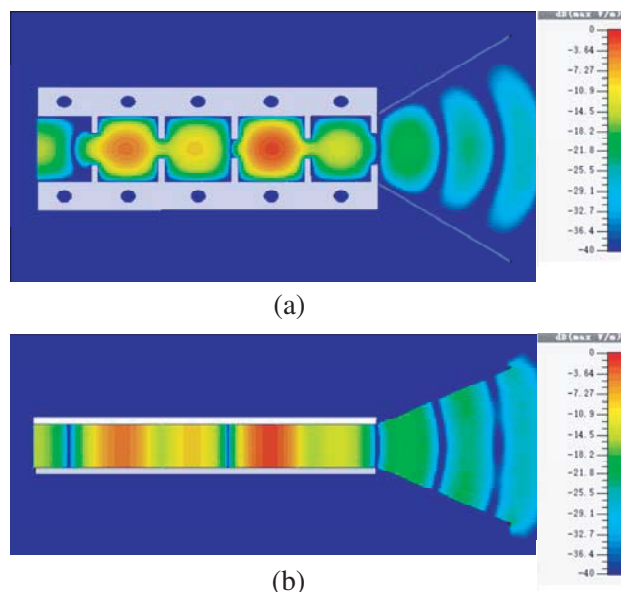


**Figure 8.** Simulated  $E$ -field magnitude distribution in CST. (a)  $H$ -plane. (b)  $E$ -plane.

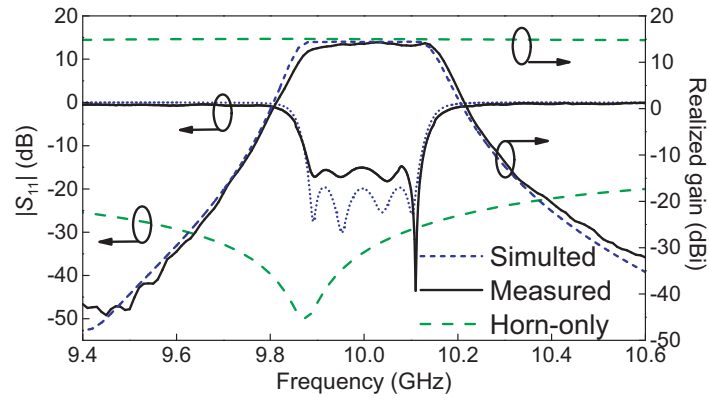


**Figure 9.** Simulated and measured  $S_{11}$  and realized gain of the antenna.

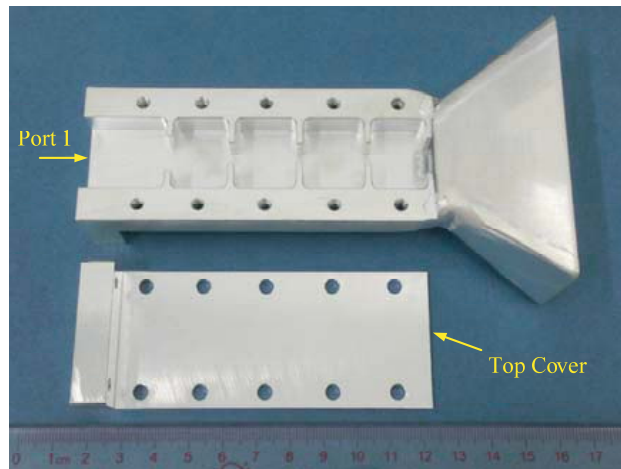


**Figure 10.** Photograph of the fabricated filtering pyramidal horn antenna.

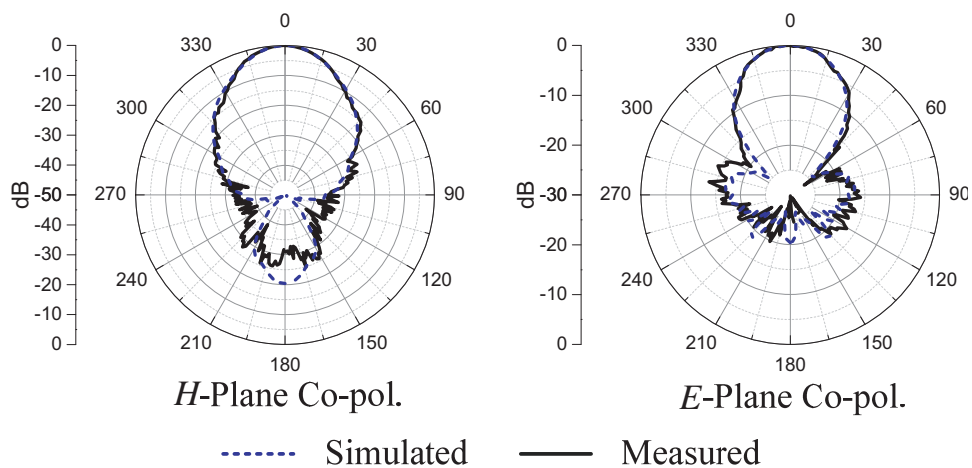


**Figure 11.** Normalized co-polarization radiation patterns of the proposed horn antenna in  $H$ -plane ( $xz$ -plane) and  $E$ -plane ( $yz$ -plane) at 10 GHz.

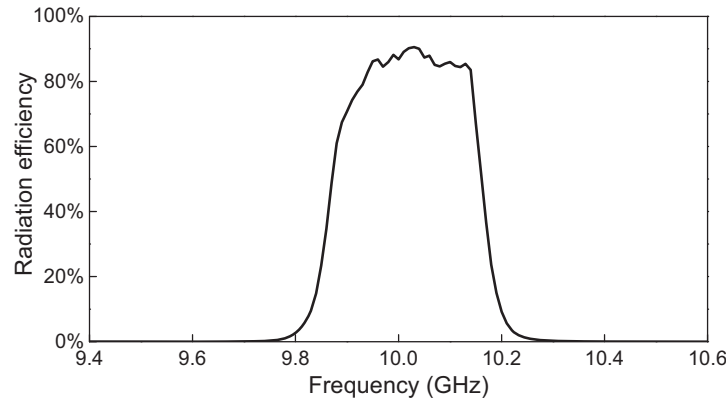


**Figure 12.** Measured radiation efficiency of the proposed horn antenna.

plane and  $E$ -plane are below  $-27.5$  dB and  $-13.5$  dB, respectively. The cross-polarized levels in  $H$ -plane and  $E$ -plane are both below  $-20$  dB in measurements and below  $-45.5$  dB and  $-44.9$  dB in simulations. The measured radiation efficiency is presented in Fig. 12, which shows that the antenna obtains a practical radiation efficiency of more than 82% from 9.94 GHz to 10.14 GHz. Both the radiation gain and efficiency illustrate great selectivity and out-of-band rejection. More radiation performance of the proposed filtering pyramidal horn antenna is summarized in Table 1.

**Table 1.** Summary of the pyramidal horn antenna performance.

Para.	HP (deg.)		SLL (dB)		Cross-Pol. (dB)	
	Sim.	Mea.	Sim.	Mea.	Sim.	Mea.
$H$	30	30.3	$-20.4$	$-27.3$	$-45.5$	$-20$
$E$	38	37.5	$-16.7$	$-13.5$	$-44.9$	$-20$

#### 4. CONCLUSION

This paper has presented an X-band waveguide filtering pyramidal horn antenna. The filtering function is a fourth order standard Chebyshev equal-ripple response. The external/radiation quality factor and coupling coefficients have been extracted to synthesize the filtering antenna. The dimensions of the pyramidal horn are designed using Cozzens's method and further optimized by simulation. Finally, the proposed antenna is fabricated and measured for experimental verification. Good agreement between the simulated and measured results is obtained. This filtering antenna is practical in X-band wireless communication systems.

#### ACKNOWLEDGMENT

This work was supported in part by the National Natural Science Foundation of China under Grant 61571194, in part by the Project of the Pearl River Young Talents of Science and Technology in Guangzhou under Grant 201610010095, and in part by the Fundamental Research Funds for the Central Universities under Grant 2018ZD07.

#### REFERENCES

1. Yusuf, Y. and X. Gong, "Compact low-loss integration of high-Q 3-D filters with highly efficient antennas," *IEEE Trans. Microw. Theory Tech.*, Vol. 59, No. 4, 857–865, Apr. 2011.

2. Yusuf, Y., H. T. Cheng, and X. Gong, "Co-designed substrate-integrated waveguide filters with patch antennas," *IET Microw. Antennas Propag.*, Vol. 7, No. 7, 493–501, Jul. 2013.
3. Chu, H., J. X. Chen, S. Luo, and Y. X. Guo, "A millimeter-wave filtering monopulse antenna array based on substrate integrated waveguide technology," *IEEE Trans. Antennas Propag.*, Vol. 64, No. 1, 316–321, Jan. 2016.
4. Lin, C.-K. and S.-J. Chung, "A compact filtering microstrip antenna with quasi-elliptic broadside antenna gain response," *IEEE Antennas Wireless Propag. Lett.*, Vol. 10, 381–384, Apr. 2011.
5. Lin, C.-K. and S.-J. Chung, "A filtering microstrip antenna array," *IEEE Trans. Microw. Theory Tech.*, Vol. 59, No. 11, 2856–2863, Nov. 2011.
6. Wu, W.-J., Y.-Z. Yin, Z.-Y. Zhang, and J.-J. Xie, "A new compact filter-antenna for modern wireless communication systems," *IEEE Antennas Wireless Propag. Lett.*, Vol. 10, 1131–1134, Oct. 2011.
7. Chen, X. W., F. X. Zhao, L. Y. Yan, and W. M. Zhang, "A compact filtering antenna with flat gain response within the passband," *IEEE Antennas Wireless Propag. Lett.*, Vol. 12, 857–860, Jul. 2013.
8. Yang, Y. and M. J. Lancaster, "Waveguide slot antenna with integrated filters," *ESA Workshop on Antennas for Space Applications*, 48–54, Noordwijk, Netherlands, Oct. 2010.
9. Chen, F. C., H. T. Hu, R. S. Li, Q. X. Chu, and M. J. Lancaster, "Design of filtering microstrip antenna array with reduced sidelobe level," *IEEE Trans. Antennas Propag.*, Vol. 65, No. 2, 903–908, Feb. 2017.
10. Zhang, B. H. and Q. Xue, "Filtering antenna with high selectivity using multiple coupling paths from source/load to resonators," *IEEE Trans. Antennas Propag.*, Vol. 66, No. 8, 4320–4325, May 2018.
11. Mahmud, R. H. and M. J. Lancaster, "High-gain and wide-bandwidth filtering planar antenna array-based solely on resonators," *IEEE Trans. Antennas Propag.*, Vol. 65, No. 5, 2367–2375, May 2017.
12. Chen, F. C., J. F. Chen, Q. X. Chu, and M. J. Lancaster, "X-band waveguide filtering antenna array with non-uniform feed structure," *IEEE Trans. Microw. Theory Tech.*, Vol. 65, No. 12, 4843–4850, Dec. 2017.
13. Balanis, C. A., *Antenna Theory-Analysis and Design*, 3rd edition, John Wiley & Sons, Inc., Hoboken, New Jersey, 2005.
14. Bilotti, F., L. D. Palma, D. Ramaccia, and A. Toscano, "Self-filtering low-noise horn antenna for satellite applications," *IEEE Antennas Wireless Propag. Lett.*, Vol. 11, 354–357, Apr. 2012.
15. Barbuto, M., F. Trotta, F. Bilotti, and A. Toscano, "Horn antennas with integrated notch filters," *IEEE Trans. Antennas Propag.*, Vol. 63, No. 2, 781–785, Feb. 2015.
16. Lancaster, M. J., *Passive Microwave Device Applications of High-temperature Superconductors*, Cambridge Univ. Press, Cambridge, UK, 1997.
17. Hong, J. S. and M. J. Lancaster, *Microstrip Filters for RF/Microwave Applications*, Wiley, New York, NY, USA, 2001.
18. Cozzens, D. E., "Tables ease horn design," *Microwaves*, 37–39, Mar. 1966.